



**HAL**  
open science

## **Mycobacterium abscessus alkyl hydroperoxide reductase C promotes cell invasion by binding to tetraspanin CD81**

Jona Karam, Fabien Blanchet, Éric Vivès, Prisca Boisguérin, Yves-Marie Boudehen, Laurent Kremer, Wassim Daher

### ► To cite this version:

Jona Karam, Fabien Blanchet, Éric Vivès, Prisca Boisguérin, Yves-Marie Boudehen, et al.. Mycobacterium abscessus alkyl hydroperoxide reductase C promotes cell invasion by binding to tetraspanin CD81. *iScience*, 2023, 26 (2), pp.106042. 10.1016/j.isci.2023.106042 . hal-04004632

**HAL Id: hal-04004632**

**<https://hal.science/hal-04004632>**

Submitted on 25 Feb 2023

**HAL** is a multi-disciplinary open access archive for the deposit and dissemination of scientific research documents, whether they are published or not. The documents may come from teaching and research institutions in France or abroad, or from public or private research centers.

L'archive ouverte pluridisciplinaire **HAL**, est destinée au dépôt et à la diffusion de documents scientifiques de niveau recherche, publiés ou non, émanant des établissements d'enseignement et de recherche français ou étrangers, des laboratoires publics ou privés.

# **Mycobacterium abscessus alkyl hydroperoxide reductase C promotes cell invasion by binding tetraspanin CD81**

Jona Karam,<sup>1</sup> Fabien P. Blanchet,<sup>1,3</sup>Éric Vive`s,<sup>2</sup> Prisca Boissgue`rin,<sup>2</sup> Yves-Marie Boudehen,<sup>1</sup> Laurent Kremer,<sup>1,3,\*</sup> and Wassim Daher<sup>1,3,4,\*</sup>

<sup>1</sup> Centre National de la Recherche Scientifique UMR 9004, Institut de Recherche en Infectiologie de Montpellier (IRIM), Université de Montpellier, 1919 Route de Mende, 34293 Montpellier, France

<sup>2</sup> PhyMedExp, University of Montpellier, INSERM U1046, CNRS UMR, 9214 Montpellier, France

<sup>3</sup> INSERM, IRIM, 34293 Montpellier, France

<sup>4</sup> Lead contact

**\*Correspondence:**

[laurent.kremer@irim.cnrs.fr](mailto:laurent.kremer@irim.cnrs.fr) (L.K.), [wassim.daher@irim.cnrs.fr](mailto:wassim.daher@irim.cnrs.fr) (W.D.)

# SUMMARY

*Mycobacterium abscessus* (Mab) is an increasingly recognized pulmonary pathogen. How Mab is internalized by macrophages and establishes infection remains unknown. Here, we show that Mab uptake is significantly reduced in macrophages pre-incubated with neutralizing anti-CD81 antibodies or in cells in which the large extracellular loop (LEL) of CD81 has been deleted. Saturation of Mab with either soluble GST-CD81-LEL or CD81-LEL-derived peptides also diminished internalization of the bacilli. The mycobacterial alkyl hydroperoxide reductase C (AhpC) was unveiled as a major interactant of CD81-LEL. Pre-exposure of macrophages with soluble AhpC inhibited mycobacterial uptake whereas overexpression of AhpC in Mab enhanced its internalization. Importantly, pre-incubation of macrophages with anti-CD81-LEL antibodies inhibited phagocytosis of AhpC-coated beads, indicating that AhpC is a direct interactant of CD81-LEL. Conditional depletion of AhpC in Mab correlated with decreased internalization of Mab. These compelling data unravel a previously unexplored role for CD81/ AhpC to promote uptake of pathogenic mycobacteria by host cells.

# INTRODUCTION

Non-tuberculous mycobacteria (NTM) are widely distributed in water pipes and soil environment.<sup>1</sup> They are acquired through the environment and can also be transmitted by aerosolization and subsequent inhalation from one person to another, particularly in immunocompromised individuals or in cystic fibrosis patients.<sup>2</sup> NTM lung disease is becoming more common and accounts for the majority of clinical cases of NTM infection.<sup>3</sup> Despite that NTM infection can affect practically every organ, pulmonary infection remains the most common clinical manifestation.<sup>4</sup> NTM are split into two groups based on their growth rate: fast growing and slow-growing.<sup>5</sup> Among these, *M. abscessus* (Mab) represents the most virulent fast-growing species, responsible for pulmonary and extra-pulmonary infections, primarily skin infections, and is commonly associated with nosocomial infections.<sup>6</sup> Mab can infect, survive, and replicate in a variety of cell types.<sup>7</sup> Endothelial epithelial cells, fibroblasts, antigen-presenting cells such as macrophages, dendritic cells, and neutrophils have been identified as potential Mab host cells.<sup>8–14</sup> Mab is found in macrophages where it manages to multiply, in contrast to other fast-growing NTM or non-pathogenic species, which are naturally cleared by macrophages.<sup>15–17</sup> The infection process begins when bacterial products, known as pathogen-associated molecular patterns (PAMP), engage with pattern recognition receptor (PRR), such as Toll-like receptors (TLR) or C-type lectins present in the plasma membrane.<sup>18</sup> PAMP binding activates either permissive or restrictive signaling pathways, which is followed by phagocytosis.<sup>19</sup> Phagocytosis of mycobacteria usually results in the formation of phagosomes, which mature and eventually fuse with lysosomes to form phagolysosomes, where microbial destruction occurs.<sup>20</sup> Mab not only survives, but also replicates within macrophages, limiting phagosome maturation and, as a result, lysosome fusion.<sup>15,21</sup> Thus, understanding the interactions between the host and the pathogen is crucial for the development of host-directed treatments that can prevent bacterial

uptake. However, PRR that contribute to the early interaction between Mab and the macrophage are poorly characterized.

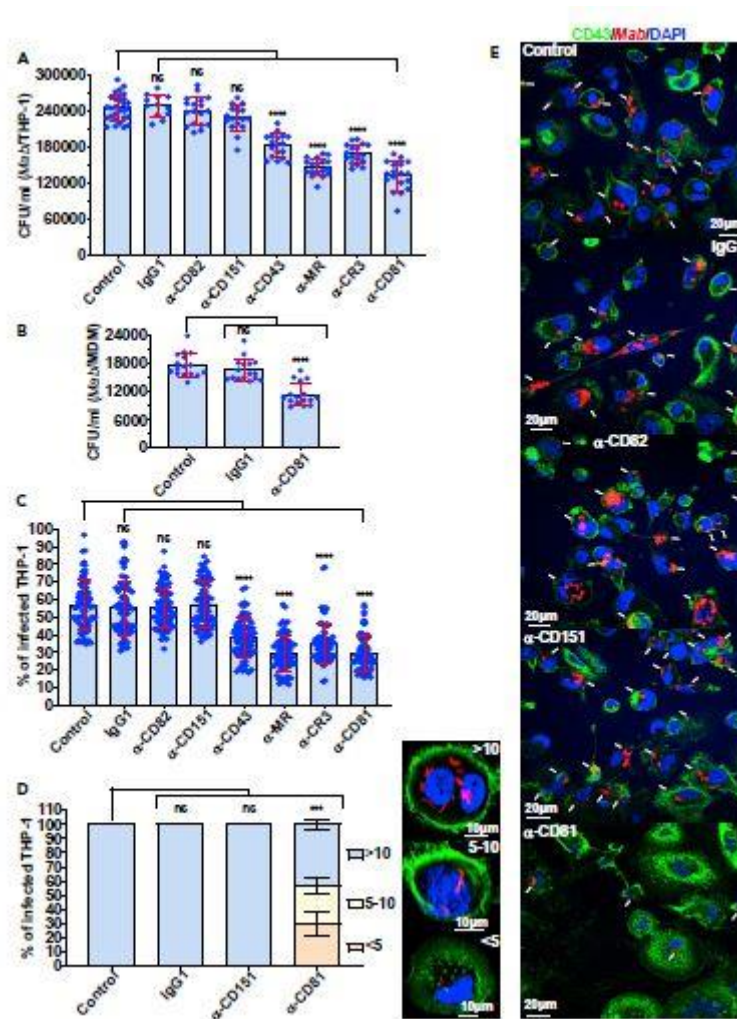


**Figure 1. Internalization of Mab by macrophages requires tetraspanin CD81**

(A and B) Uptake of Mab is reduced in THP-1 macrophages (A) and primary human macrophages (B) pre-treated with neutralizing antibodies raised against CD43, MR, CR3 or CD81. Macrophages were lysed with 1% Triton X-100 and then successive dilutions of the different suspensions were prepared and plated on LB agar before CFU counting. Data are mean values GSD for six (A) or four (B) independent experiments, each time in triplicate (A) or quadruplicate (B),  $n = 18$  (A) or 16 (B). One-tailed Tukey's test: ns, non-significant  $> 0.05$ ,  $***p < 0.0001$ . (C) Blocking CD43 or MR or CR3 or CD81 receptors with neutralizing antibodies significantly reduces the percentage of Mab-infected THP-1 macrophages. Quantification of the percentage of host cells containing bacilli was performed using an epifluorescence microscope. Images were acquired focusing on the combined signals (CD43 in green and Mab in red) and scoring for the presence or absence of bacilli in macrophages using ImageJ. Data are mean values GSD for four independent experiments ( $n = 80$  fields). One-tailed Tukey's test: ns, non-significant  $> 0.05$ ,  $***p < 0.001$ . (D) Percentage of Mab-infected THP-1 macrophage categories after pre-treatment with neutralizing antibodies raised against CD151 or CD81. The images illustrate a macrophage  $< 5$  bacilli, 5 to 10 bacilli or  $> 10$  bacilli (upper right). The nuclei were stained with DAPI (blue) and the surface of macrophages was stained with anti-CD43 antibodies (green). Values are means GSD for three independent experiments performed each time in triplicate ( $n = 900$  infected macrophages). One-tailed non-paired t-test: ns, non-significant  $> 0.05$ ,  $***p < 0.001$ . (E) Five immunofluorescent fields were taken at 3 h post-infection using a confocal microscope (403 magnification), showing the macrophages infected with the Mab (in red) following pre-treatment with indicated antibodies. The nuclei are in blue and the CD43 protein associated with the plasma membrane of macrophages is in green. White arrows indicate Mab inside the cells.

Tetraspanins belong to a superfamily of glycoproteins, which span the membrane four times and possess a small (SEL) and a large extracellular loop (LEL).<sup>22</sup> These proteins display a wide panel of cellular functions (adhesion, motility, and fusion) and are related to infection by a variety of human pathogens, including viruses, parasites and bacteria.<sup>22</sup> Humans possess 33 tetraspanins, with most cells expressing simultaneously multiple members of this family of proteins.<sup>23</sup> The LEL domains show the largest sequence diversity and are involved in member-specific functions.<sup>24</sup> In addition, LEL domains can be recombinantly produced with a conserved biological activity. Tetraspanin actions are based on their capacity to connect with other molecules present in the membrane, generating functional assemblies known as tetraspanin-enriched microdomains (TEM).<sup>25</sup> There is mounting evidence that viruses, parasites, and bacteria can bind to and infiltrate host cells using various tetraspanins.<sup>22</sup> CD81 is a hepatitis C virus receptor<sup>26</sup> that can also influence HIV-1 membrane fusion and viral clustering at the viral synapse.<sup>27</sup> It is also necessary for the infection of hepatocytes by Plasmodium.<sup>28</sup> Following infection of epithelial cells by *Listeria*, CD81 is attracted to the site of bacterial entrance.<sup>29</sup> However, a possible CD81-dependent mechanism underlying mycobacterial entrance into macrophages or lung epithelial cells remains yet to be established.

The goal of this study consisted to stimulate the discovery of a hitherto unknown ligand-receptor interaction that mediates Mab infection in macrophages and lung epithelial cells. We evaluated whether CD81 may represent a PRR that favors the internalization of Mab inside human macrophages and lung epithelial cells. The combination of biochemical and mass spectrometry techniques led to the identification of AhpC as a strong mycobacterial candidate acting as a CD81-specific PAMP. Subsequent genetic studies and cellular biology approaches were conducted to confirm and validate the importance of the CD81/AhpC interaction in promoting the recognition and internalization of Mab by macrophages.

## RESULTS

### **CD81 is required for invasion of macrophages by Mab**

Tetraspanin CD81 is expressed on the host cell surface and is identified as a receptor for the hepatitis C virus (HCV) E2 envelope glycoprotein.<sup>26</sup> In addition, *Plasmodium yoelii* and *Plasmodium falciparum* sporozoites utilize a specific CD81-dependent pathway to enter hepatocytes.<sup>28</sup> We, thus, addressed whether CD81 is involved in *M. abscessus* (Mab) uptake, subsequently leading to macrophage infection. The requirement of CD81 for the internalization of Mab by macrophages was suggested using neutralizing monoclonal antibodies specifically directed against CD81-LEL (Figure 1A). Results show that pre-treatment of human THP-1 cells with the antibodies before Mab infection effectively inhibited bacilli invasion of macrophages and significantly reduced the intracellular bacterial burden. As negative controls, IgG1 isotype or monoclonal antibodies raised against tetraspanins CD82 and CD151, had no impact on Mab uptake by macrophages (Figure 1A). Unexpectedly, neutralization of CD81 reduced Mab invasion to the same extent than neutralization of CD43, mannose receptor (MR) and complement receptor 3 (CR3) (Figure 1A), known as major PRR participating in the invasion of *Mycobacterium tuberculosis*.<sup>30–34</sup> Similar results were obtained when assaying primary human monocyte-derived macrophages (MDM) (Figure 1B).

In parallel, quantification of infected macrophages revealed a marked reduction in the percentage of Mab-containing cells when pre-treated with anti-CD43, MR, CR3, and CD81 antibodies (Figures 1C, 1E, and S1). This was not observed in THP-1 cells either pre-incubated with the IgG1 isotype control, anti-CD82 or anti-CD151 antibodies (Figures 1C and 1E). To further assess the consequences of this invasion defect, infected macrophages were classified into three categories at 3 hours post-infection (hpi) based on their bacterial content: weakly infected (<5 bacilli/cell), moderately infected (5–10 bacilli/cell), and heavily infected (>10 bacilli/cell) (Figure 1D). The results indicate that blocking CD81, but not CD151, profoundly increased the proportion of the weakly infected category while reducing the percentage of heavily infected cells (Figures 1D and 1E). Together, this suggests that CD81 is involved in Mab uptake by macrophages.

### **Peptide competition with CD81-LEL reduces mycobacterial entry into macrophages**

To assess whether CD81 acts as a macrophage receptor for the bacilli through its LEL domain, soluble GST-tagged CD81-LEL fusion protein (GST-CD81-LEL) produced in *Escherichia coli* was used in competition assays with Mab in THP-1 cells. CD151-LEL was also produced and included as a control. Bacteria were pre-incubated with the two GST-LEL proteins (Figure S2A), separately for 3 h at 37°C before infection. In contrast to GST-CD151-LEL, pre-incubation with GST-CD81-LEL significantly reduced both the intracellular bacterial burden (Figure 2A) and the percentage of Mab-infected THP-1 cells (Figures 2B, 2D, and S2B), relative to the GST control. A marked increase in the proportion of the low-infected macrophage category was also observed when bacilli were pre-incubated with GST-CD81-LEL, but not with GST-CD151-LEL or GST alone (Figures 2C and 2D). This inhibitory effect on bacterial entry was also dose-dependent, supporting both a qualitative and quantitative effect of the fusion protein-mediated competition (Figures 2A and 2B).

Next, two short peptides (810 and 910) exposed and located between the 3 cysteine residues (Cys157, Cys175 and Cys190) found in CD81-LEL (Figures S3A and S3B) were synthesized in their linear (SH) or cyclic (SS) forms and tested for their activity to influence Mab uptake by THP-1 cells. A scrambled peptide (SCR), consisting of the same amino acids in random order, was included as an internal control. Mab were pre-incubated with different concentrations of peptides, ranging from 50 mM to 100 mM. Significant reductions in bacterial uptake were observed with both the 810 and 910-derived peptides (Figures 2E, 2F, and S3C). These results indicate that both the linear and cyclic forms of peptide 910 are equally effective and act at lower concentrations than peptide 810 to block mycobacterial internalization. As anticipated, bacteria pre-treated with the SCR peptide showed no reduction in their ability to invade the macrophages (Figures 2E and S3C). Collectively, these data establish the importance of the LEL short loops formed between the disulfide bridges in the interaction with the bacterial ligand(s) and required for the internalization process.

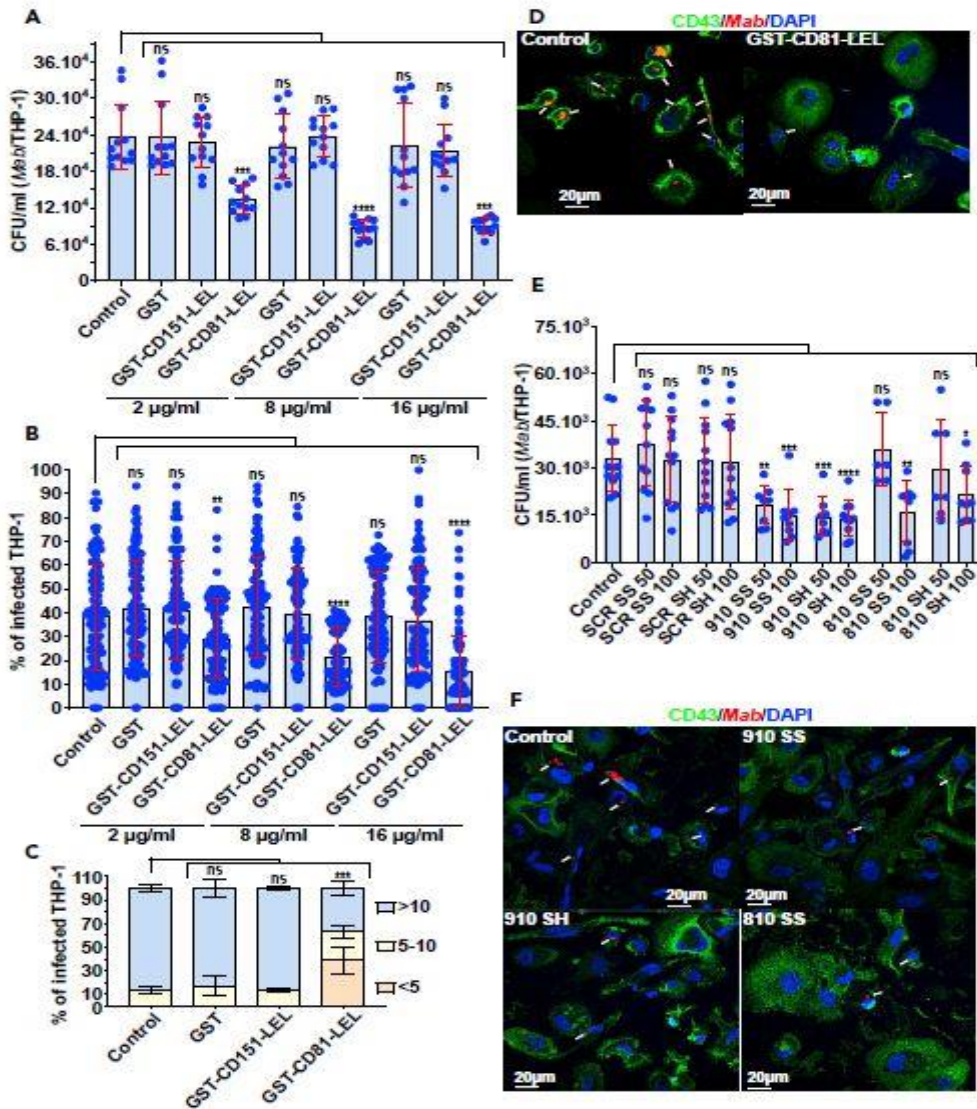


**Figure 2. Recombinant GST-CD81-LEL or CD81-LEL derived peptides reduce Mab internalization by macrophages**

(A) Uptake of Mab is reduced in THP-1 macrophages pre-treated with recombinant GST-CD81-LEL at different concentrations (2, 8 and 16 mg/mL). Macrophages were lysed with 1% Triton X-100 and serial dilutions were plated before CFU counting. Data are mean values GSD for four independent experiments (each time in triplicate) ( $n = 12$ ). One-tailed Tukey's test: ns, non-significant  $> 0.05$ , \*\*\* $p < 0.001$ , \*\*\*\* $p < 0.0001$ . (B) Pre-incubation of Mab with different concentrations of recombinant GST-CD81-LEL (2, 8 and 16 mg/mL) significantly reduces the bacterial uptake and percentage of infected macrophages. Quantification of the percentage of cells containing bacilli was performed as in Figure 1C. Data are mean values GSD for six independent experiments ( $n = 120$  fields). One-tailed Tukey's test: ns, non-significant  $> 0.05$ , \*\* $p < 0.01$ , \*\*\*\* $p < 0.0001$ . (C) Percentage of macrophage categories after pre-treatment with recombinant GST-CD81-LEL at 16 mg/mL. The number of bacilli/macrophage drops when bacilli were pre-incubated with CD81-LEL. Values are means G SD for three independent experiments performed each time in triplicate ( $n = 900$  infected macrophages). One-tailed non-paired t test: ns, non-significant  $> 0.05$ , \*\*\* $p < 0.001$ . (D) Two immunofluorescent fields taken at 3 h post-infection using a confocal microscope (403 magnification), showing the macrophages infected with Mab (in red) after pre-treatment with GST-CD81-LEL. The nuclei are shown in blue, the CD43 protein associated with the plasma membrane of macrophages is in green. White arrows indicate Mab inside the macrophage. (E) Uptake of Mab is reduced in macrophages when bacilli were pre-treated with CD81-LEL-derived peptides (810 and 910) either in a linear form (reduced SH) or in a cyclic form (oxidized SS) at 50 or 100 mM. A scrambled (SCR) peptide in its reduced and oxidized form is used as negative control. To determine the number of internalized with 1% Triton X-100 and lysates were plated on LB agar before CFU

counting. Data are mean values GSD for four independent experiments performed each time in triplicate (n = 12). One-tailed Tukey's test: ns, non-significant >0.05, \*p < 0.1, \*\*p < 0.01, \*\*\*p < 0.001, \*\*\*\*p < 0.0001.

(F) Four immunofluorescent fields taken at 3 h post-infection using a confocal microscope (403 magnification), showing the macrophages infected with Mab (in red) after pre-treatment with CD81-LEL-derived or SCR peptides. The nuclei are shown in blue, the CD43 protein associated with the plasma membrane of macrophages is in green. White arrows indicate Mab inside the cells.

## Deletion of the CD81-LEL reduces bacterial internalization in lung epithelial cells

To confirm the role of CD81-LEL in Mab internalization, CRISPR/Cas9-mediated genome editing was applied to A549 lung epithelial cells, yielding to A549-CD81-LEL-KO cells. A guide RNA targeting the exon 4 of Cd81 gene just upstream of the LEL coding DNA region was designed. Guide RNA (sgRNA) sequence targeting Cd81 was designed and cloned into the LentiGuide-Puro (Figure S4A). 35 Viral particles generated in HEK293T cells were used to knock-out the LEL of Cd81 genes specifically in A549 cells by lentiviral transduction and single-cell cloning (Figure S4A). A549-CD81-LEL-KO cells were further sorted by flow cytometry and isolated into a single cell by limiting dilution. One single clone was expanded and selected for further analysis. Specific introduction of indels at the sgRNA cut site in A549 cells was validated by PCR and complete sequencing of Cd81 open reading frame (Figure S4B). Cloning of the PCR products obtained from the cDNA prepared from clone A549-CD81-LEL-KO cells into the TOPO vector, followed by sequencing, revealed the existence of two different deletions, presumably representing two different genomic repairs occurring at the 2 Cd81 alleles (Figure S4B). The first one exhibited a 5-bp deletion in the translated region of Cd81 gene, which would generate a chimeric and short protein lacking LEL (Figures S4B and S4C), whereas the second one revealed a 20-bp deletion that also generated a chimeric and truncated protein lacking the LEL (Figures S4B, and S4C). Flow cytometry and immunofluorescence analyses using anti-CD81-LEL antibodies confirmed the absence of CD81-LEL expression at the cell surface as well as intracellularly, when compared with the unedited controls (Figures 3A and 3B). No defect in the expression levels of tetraspanins CD9 and CD63 were observed in A549-CD81-LEL-KO as compared to A549-WT cells (Figures 3A and 3B). Expression of the truncated CD81 protein was confirmed by sequencing analysis. Overall, this underscores the successful and specific deletion of CD81-LEL in the A549-CD81-LELKO cells. Importantly, infection of A549-CD81-LEL-KO cells showed a significant decrease in the number of internalized Mab as compared to WT A549 cells (Figures 3C and 3E). Quantitative analysis revealed also a marked reduction in the percentage of Mab-containing cells in the absence of CD81-LEL (Figures 3D and 3E). These results are fully consistent with those from the pre-treatment experiments using either neutralizing anti-CD81 antibodies or recombinant GST-LEL fusion proteins (Figures 1 and 2). They demonstrate that surface-associated CD81 plays a crucial role in internalization of Mab by macrophages and lung epithelial cells in a CD81-LEL-dependent manner.

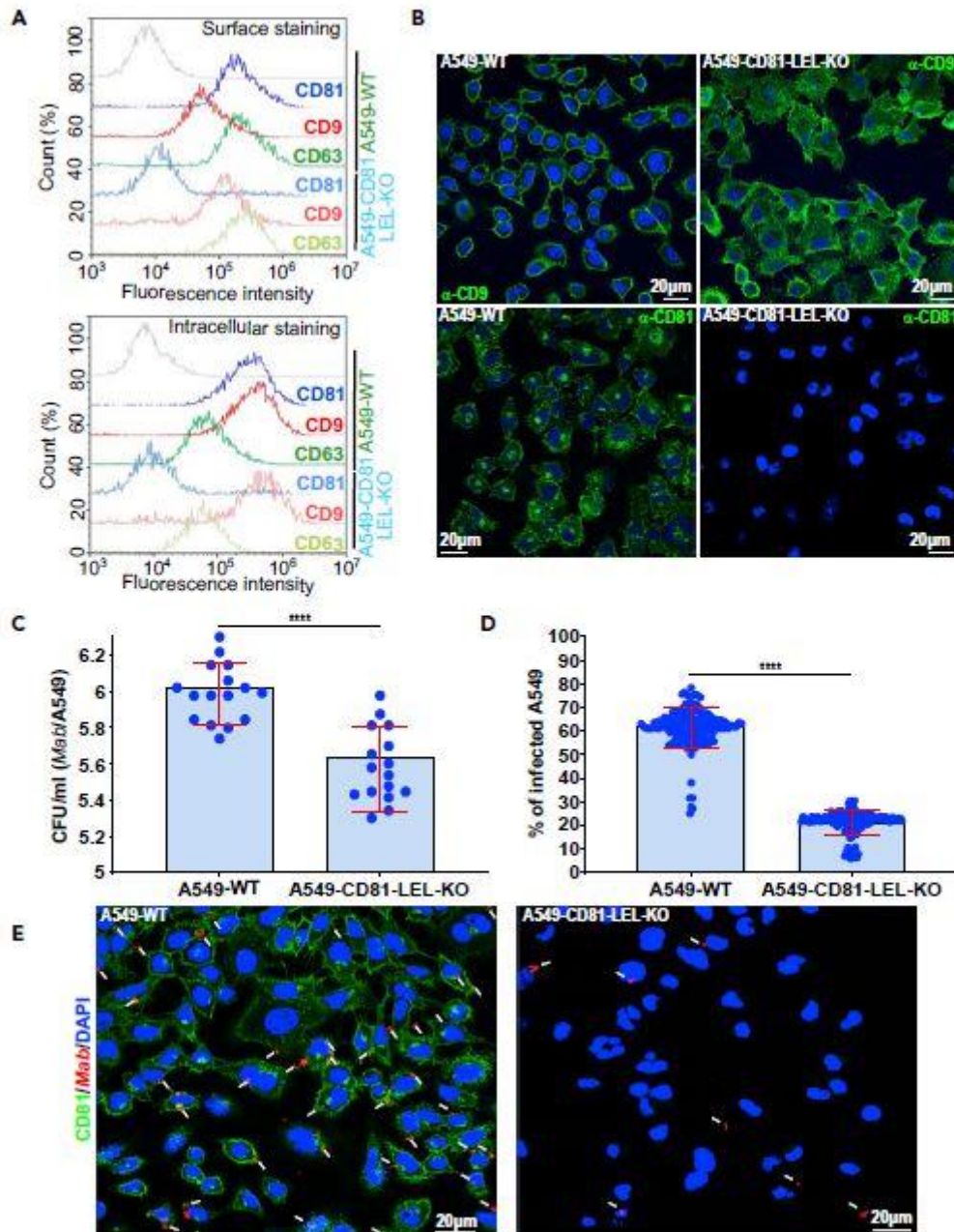


**Figure 3. Deletion of CD81-LEL in lung epithelial cells reduces internalization of bacilli and intracellular bacterial loads**

(A) A549-WT or A549-CD81-LEL-KO cells were harvested and fixed in 2% paraformaldehyde before washing and incubated with indicated primary antibodies, followed by staining with Alexa Fluor 647-coupled secondary antibodies in non-permeabilizing (surface staining) or permeabilizing (intracellular staining) buffer. Cells were then washed and processed through a Novocyt ACEA cytometer. Surface staining (upper inset) and intracellular staining (lower inset) are represented as histogram overlays for each tetraspanin expression in both cell types (CD81 in blue; CD9 in red; CD63 in green). The staining control was done with incubation of secondary antibodies alone (gray curves). (B) Localization of tetraspanins CD9 and CD81 (green staining) in A549\_WT cells and in A549-CD81-LEL-KO cells. Because these antibodies are directed against the LEL, no CD81 signal is detected in A549-CD81-LEL-KO cells. (C) Impact of CD81-LEL disruption in A549 cells on the internalization of Mab. CFUs were determined at 3 h post-infection, as described previously. Data are the means GSD values for four independent experiments performed in quadruplicate (n = 16). One-tailed Tukey's test: ns, non-significant > 0.05; \*\*\*\*p < 0.0001. (D) Deletion of CD81-LEL significantly diminishes the uptake of Mab and the percentage of infected A549 cells. Quantification of the percentage of host cells containing bacilli was

performed as in Figure 1C. Data are mean values GSD for eight independent experiments (n = 160 fields). One-tailed Tukey's test: ns, non-significant > 0.05, \*\*\*\*p < 0.0001. (E) Immunofluorescence confocal microscopy fields showing A549 WT, or A549-CD81-LEL-KO cells infected with red fluorescent mycobacteria (white arrows). The cell surface is stained using anti-CD81 antibodies (green) whereas the nuclei are stained with DAPI (blue).

## Identification of CD81 ligands in *M. abscessus*

The mycobacterial protein partners possibly interacting with CD81 are not known. To uncover putative ligands in Mab, a GFP-Trap pull-down approach was developed using anti-GFP nanobodies on lysates derived from mycobacteria expressing either GFP or CD81-LEL-GFP (Figures S5A and S5B) followed by mass spectrometry analyses to identify the immunoprecipitated proteins (Figure S5C). After several washes, one-fifth of each eluate was subjected to SDS-PAGE and silver staining (Figure S5D). Although a few proteins were bound to GFP- or to CD81-LEL-GFP-coated beads, the samples showed very different profiles (Figure S5D). Mass spectrometry analysis on selected proteins which were not present in the control eluate yielded at least five unique peptides (Figure S5E). Among these, a heat shock protein (Hsp16.7), an antioxidant enzyme (AhpC), and two hypothetical proteins (MAB\_3498c and MAB\_1957) (Figure S5E). This suggests that these potential uncharacterized protein partners may participate in the interaction between Mab and CD81. We then focused on AhpC (encoded by MAB\_4408c), detected with the most unique peptides by mass spectrometry (11 versus 5 for the other candidates) and whose orthologue in *M. tuberculosis* is an alkyl hydroperoxide reductase playing a specific role in antioxidant defenses.<sup>36</sup> Subsequent validation was based on a reverse HA-Trap pull-down approach. First, a Mab strain expressing AhpC-HA under the control of the hsp60 promoter was generated and expression was checked by western blotting using anti-HA antibodies (Figure 4A). Second, bacterial lysates from the strain expressing AhpCHA were mixed with lysates from Mab strains expressing either GFP or CD81-LEL-GFP to form two total bacterial lysates, designated TBL-I and TBL-II, respectively, and incubated with beads coupled to anti HA antibodies (Figure S6). HA-Trap pull-down and subsequent western blotting using anti-GFP or anti-HA antibodies revealed the presence of CD81-LEL-GFP, GFP or AhpC-HA in the eluted fractions (Figure 4B). Importantly, a single band with the appropriate size of CD81-LEL-GFP was specifically pulled down with AhpC-HA but not with GFP alone or with Fmt-HA (a fatty acid methyltransferase from Mab), both used as negative controls (Figures 4B and 4C). This confirms the specific interaction between AhpC and CD81-LEL-GFP.

To determine whether AhpC is located in the cell wall fraction where it could exert its role as a surface adhesin to interact with CD81, sequential centrifugation/ultracentrifugation steps of total lysates from the AhpC-HA-overexpressing strain led to several fractions enriched for cell wall (CW), plasma membrane (PM) or cytosol (Cyt) proteins. SDS-PAGE followed by immunoblotting using anti-HA antibodies revealed a strong signal at 25 kDa in all fractions, in agreement with the predicted molecular weight of AhpC-HA (Figure 4D). To exclude the possibility of contaminating cytosolic proteins in the CW and PM fractions, membranes were probed with anti-His antibodies to detect the cytosolic GroEL1 protein (Figure 4D). These results support the view that AhpC is a cell wall-associated protein, thus ideally exposed to interact with CD81 (Figure 4D).

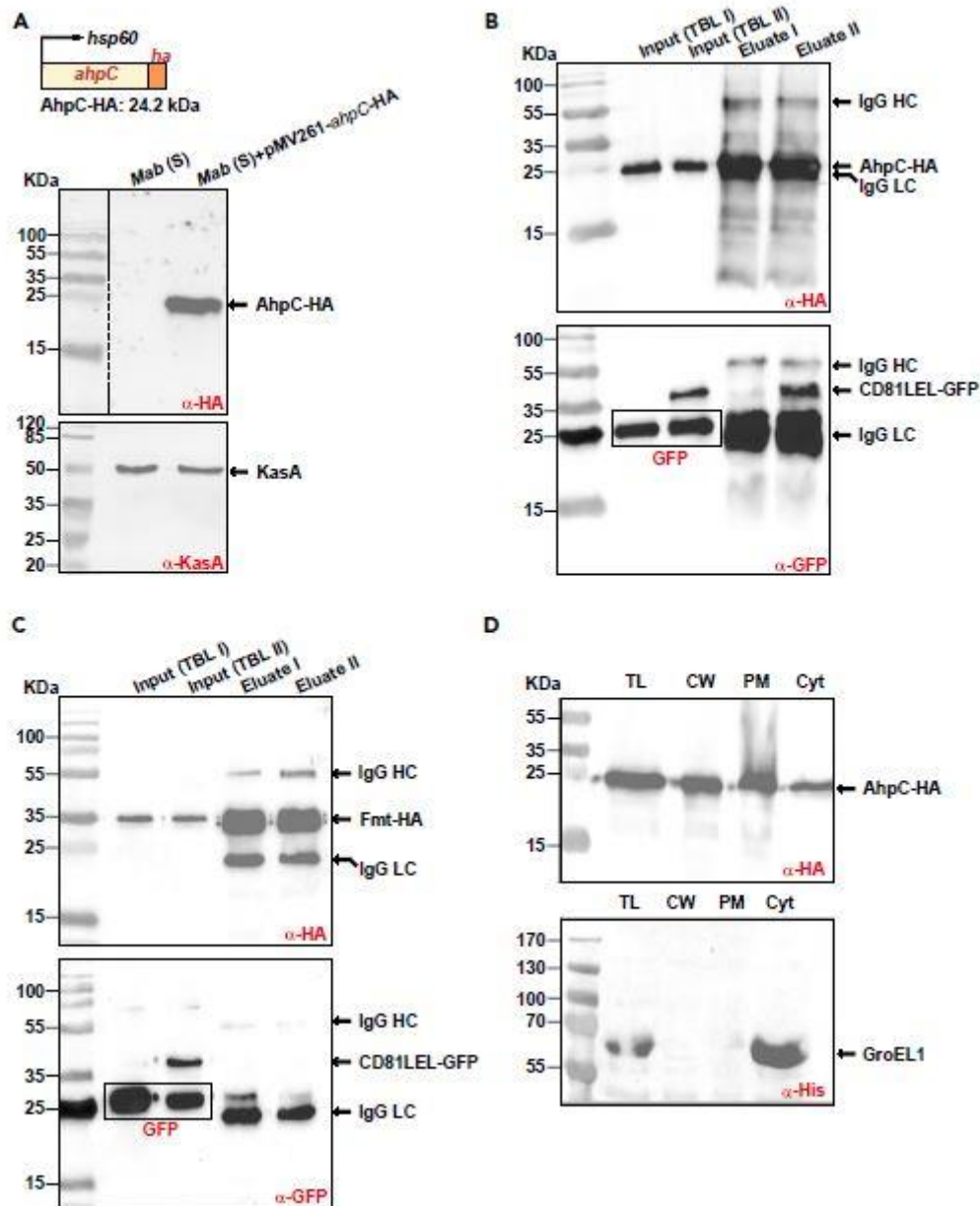


**Figure 4. AhpC interacts specifically with CD81-LEL**

(A) Overexpression of AhpC-HA in Mab. The *ahpC* (MAB\_4408c) gene was fused to HA and expressed under the control of *hsp60* promoter (see also Table S1). Upper panel: Western blotting of AhpC overexpression in Mab using anti-HA antibodies. Lower panel: The KasA protein (probed with anti-KasA antibodies) was used as a loading control. (B) Interaction of CD81-LEL-GFP with Mab AhpC. Co-immunoprecipitation of the complex CD81-LEL-GFP/AhpC-HA was carried out with anti-HA antibodies from Mab extracts. Immunoprecipitates from control (Mab co-expressing GFP and AhpC-HA; lane 3) or from Mab co-producing CD81-LEL-GFP and AhpC-HA (lane 4) were eluted and immunoblotted using either anti-HA (upper blot) or anti-GFP (lower blot) antibodies. Lanes 1 and 2 allow to detect AhpC-HA or GFP or CD81-LEL-GFP proteins in the TBL I and TBL II bacterial soluble extracts before proceeding to the immunoprecipitation experiments using beads coated with anti-HA antibodies. LC: immunoglobulin light chain; HC: immunoglobulin heavy chain. (C) The Fatty acid methyltransferase (Fmt) from Mab does not interact with CD81-LEL-GFP. The experiments were conducted as indicated in (B) by replacing AhpC-HA by Fmt-HA in the assay. (D) Immunoblotting showing the localization of AhpC in different fractions: total lysate (TL), cell wall (CW), plasma membrane (PM), and cytosol (Cyt). The cytosolic marker GroEL1 was included as a control.

## **AhpC promotes Mab uptake by macrophages via CD81**

Mab AhpC and Hsp16.7, both identified by mass spectrometry (Figure S5E), were produced and purified as recombinant AhpC-63His and Hsp16.7-63His proteins from *E. coli* (Figures S7A and S7B). Fluorescent latex beads (1 μm diameter) were coated with either AhpC-63His, Hsp16.7-63His or BSA. The efficacy of coating was confirmed by SDS-PAGE/western blotting (Figures S7C and S7D) and by immunofluorescence using anti-His or anti-BSA antibodies (Figures 5A, 5B, and S7E). The effect of protein coating on beads uptake was next assessed by incubating THP-1 macrophages with the different fluorescein-labeled latex beads. Quantification of the percentage of bead-containing cells clearly demonstrated that macrophages internalized significantly more AhpC-coated beads (5- to 10-fold) than Hsp16.7-, or BSA-coated beads (Figures 5C and 5E). Strikingly, the uptake of AhpC-beads was inhibited by pre-treating macrophages with anti-CD81 antibodies but not in the presence of the IgG1 control isotype (Figures 5D and 5E). This validates the physical interaction between AhpC and CD81 to favor the internalization of the beads by macrophages. High-resolution confocal imaging also highlighted the intracellular localization of the counted beads (Figure 5E). Collectively, these findings show that mycobacterial AhpC acts as a ligand for the host CD81 and that internalization of whole bacteria by host cells is dependent on the AhpC/CD81 pair.

## **Overexpression of ahpC enhances AhpC-mediated cell entry**

Whether overproduction of AhpC interferes with bacterial invasion was tested by overexpressing *ahpC* (as well as *hsp16.7*) in Mab. For this purpose, the episomal pMV261 carrying either *hsp16.7* or *ahpC* fused to an HA-tag under the control of the *hsp60* promoter was introduced into Mab and the invasion rates of Mab\_WT, Mab\_ahpC\_OV or Mab\_hsp16.7\_OV were compared. As shown in Figure 6A, the internalization of Mab\_S\_ahpC\_OV was 2-fold higher than internalization of Mab\_WT or Mab\_hsp16.7\_OV, suggesting that AhpC is acting as a mycobacterial adhesin. To further assess the impact of AhpC on infection, THP-1 cells were pre-incubated with recombinant AhpC-His before macrophage infection with whole bacteria. Pre-treatment with 2 mg AhpC-His partially blocked internalization of the Mab\_WT and reduced infectivity by 30% as compared to untreated cells or to cells pre-incubated with recombinant Hsp16.7-His (Figures 6B and 6C).

To validate the role of CD81 in interacting with AhpC on whole bacteria, we investigated the ability of Mab\_WT and Mab\_ahpC\_OV strains to invade A549-WT and A549-CD81-LEL-KO cells. CFU determination indicates that although overproduction of AhpC in *ahpC*-OV enhances Mab internalization by A549 cells (confirming the results obtained in macrophages), the uptake of Mab\_ahpC-OV is significantly reduced in A549-CD81-LEL-KO cells as compared to the uptake of Mab\_WT in these cells (Figure 6D). This emphasizes the requirement of CD81 for optimal internalization of the AhpC-overproducing strain. Overall, these results indicate that whereas overproduction of AhpC facilitates Mab internalization, pre-incubation of cells with soluble AhpC inhibits the internalization process, thus indicating that AhpC behaves like a canonical adhesin.

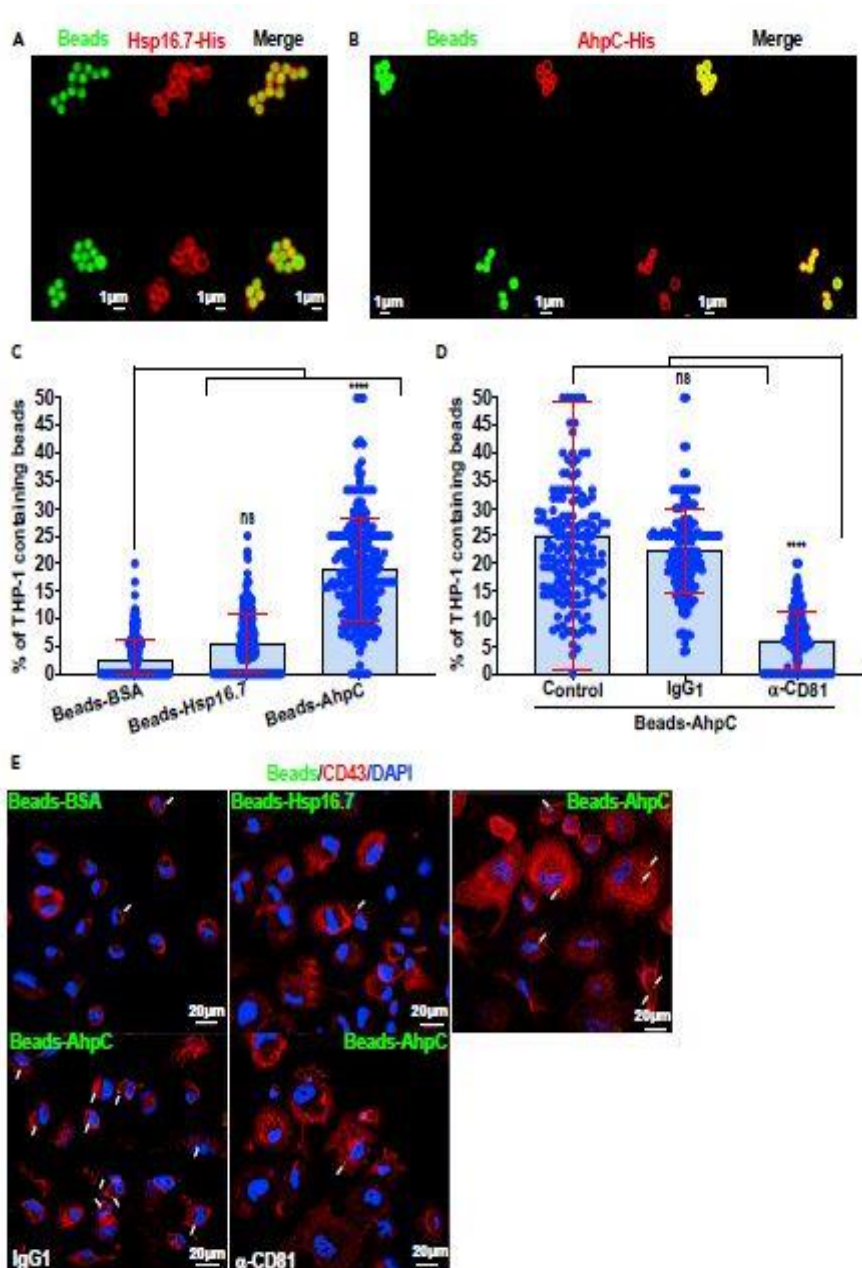


**Figure 5. AhpC interacts directly with CD81 and promotes internalization of fluorescein-tagged latex beads**

(A and B) Protein coating of fluorescein-tagged latex beads with recombinant Mab Hsp16.7-His or AhpC-His. Labeling of Hsp16.7-His or AhpC-His proteins (red) at the surface of fluorescein tagged latex beads (green) was detected using mouse anti-His antibodies and Alexa Fluor 594 conjugated goat anti-mouse secondary antibodies. (C) Ingestion of beads by THP-1 macrophages for 4 h is optimal when coated with AhpC. Data are mean values GSD for three independent experiments (each time in octuplicate) (n = 240 fields). One-tailed Tukey's test: ns, nonsignificant > 0.05, \*\*\*\*p < 0.0001. (D) Blocking CD81 with neutralizing antibodies drastically reduces the uptake of AhpC-coated beads. Data are mean values GSD for four independent experiments (each time in quadruplicate) (n = 160 fields). One-tailed Tukey's test: ns, non-significant > 0.05, \*\*\*\*p < 0.0001. (E) Representative fluorescent images showing either the efficiency of internalization and impact of neutralizing anti-CD81 antibodies on the internalization of AhpC-coupled beads by macrophages. CD43 (red), DAPI (blue) and fluorescent beads (green). White arrows indicate fluorescent beads inside macrophages.

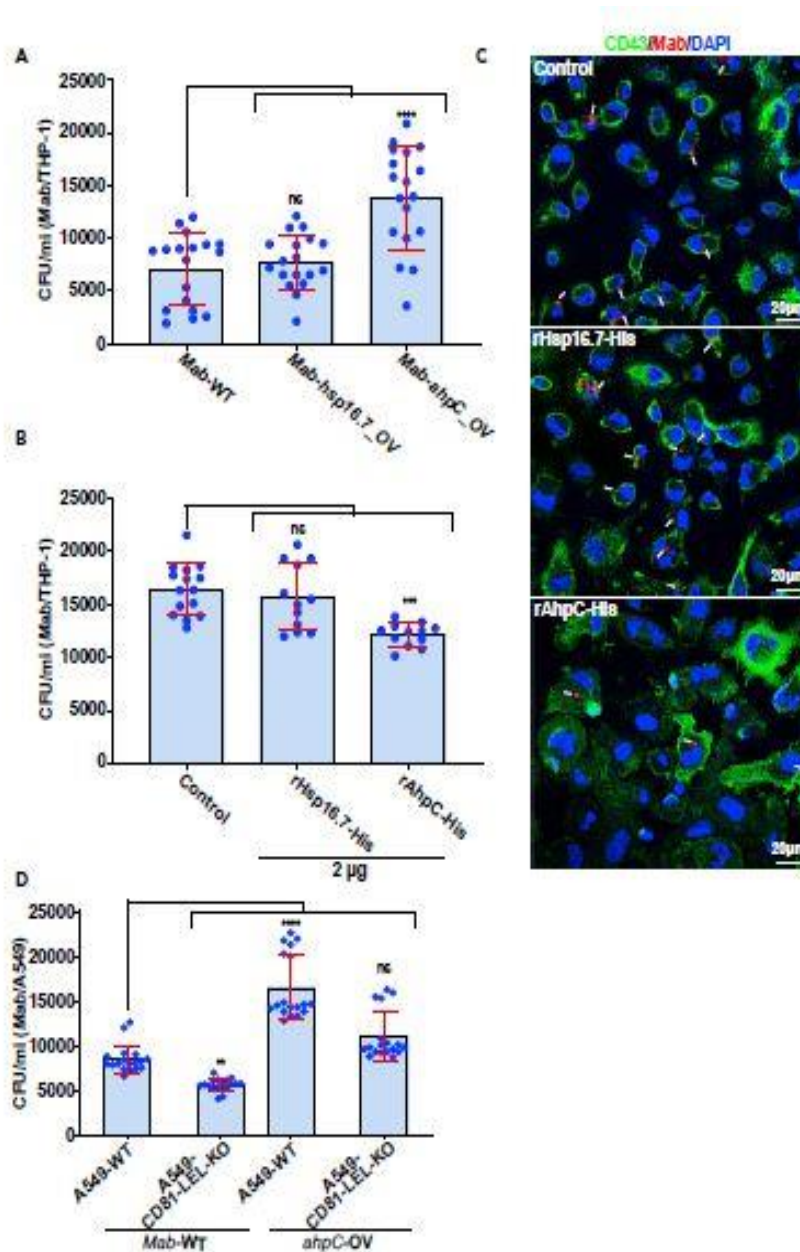


**Figure 6. Overexpression of AhpC enhances colonization of macrophages by Mab**

(A) Effect of overexpression of AhpC or Hsp16.7 on the ability of Mab to invade THP-1 macrophages (see also Table S1). CFU were calculated as reported above. Data are mean values GSD for three independent experiments, each time in sextuplicate ( $n = 18$ ). One-tailed Tukey's test: ns, non-significant  $> 0.05$ , \*\*\*\* $p < 0.0001$ . (B) Pre-treatment of THP-1 cells with 2 mg of soluble recombinant Hsp16.7-His or AhpC-His on the ability of Mab to colonize THP-1 human cells. CFU were determined as described above. Data are mean values GSD for three independent experiments, each time in triplicate ( $n = 12$ ). One-tailed Tukey's test: ns, non-significant  $> 0.05$ , \*\*\* $p < 0.001$ . (C) Three immunofluorescent fields taken at 3 hpi using a confocal microscope (403 magnification), showing the macrophages infected with Mab (in red) after pre-treatment of THP-1 cells with Hsp16.7-His or AhpC-His recombinant proteins. Nuclei are in blue and the cell surface is in green. White arrows indicate mycobacteria inside macrophages. (D) Overexpression of AhpC enhances entry of bacilli into A549-WT in a CD81-LEL-dependent manner. CFU were assessed at 3 hpi as outlined earlier. Data are mean values GSD for three independent experiments, each time in sextuplicate ( $n = 18$ ). One-tailed Tukey's test: ns, non-significant  $> 0.05$ , \*\* $p < 0.01$ , \*\*\*\* $p < 0.0001$ .

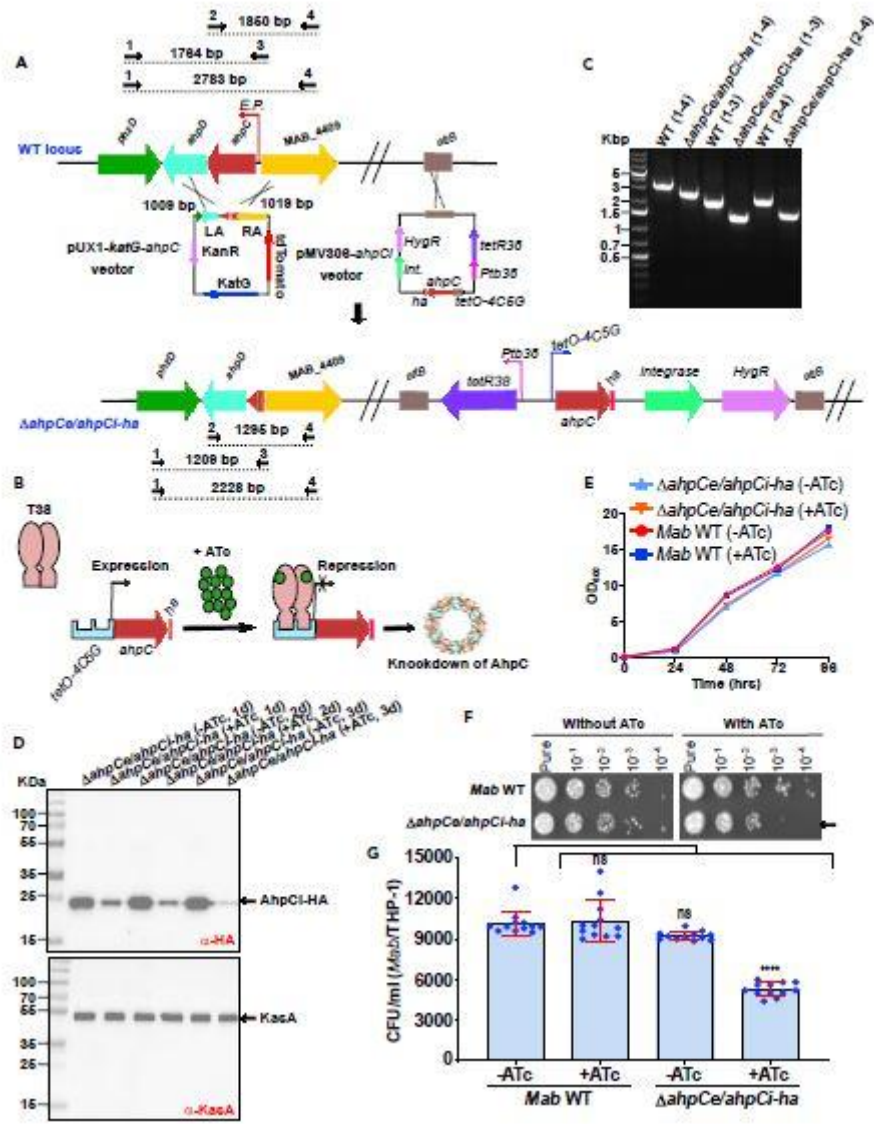


**Figure 7. Internalization of Mab by macrophages requires the AhpC adhesin**

(A) Schematic illustration of the Mab *ahpC* conditional knock-out strategy (see also Table S1). Mab was transformed with the regulatory, ha-tagged *ahpCi* plasmid (pMV306-*ahpCi*) to generate a merodiploid bacterial strain. The pMV306-*ahpCi* vector was integrated into the *attB* site by single homologous recombination. The pMV306-*ahpCi* contains the integrase gene (*int*), the hygromycin resistance cassette (*HygR*), the *tetR38* repressor under the control of the *Ptb38* promoter, and the C-terminal ha-tagged *ahpC* gene under the control of the inducible *tetO-4C5G* promoter. The single merodiploid clone was then transformed with pUX1-*katG-ahpC* to remove the endogenous *ahpC* gene (*ahpCe*) by double homologous recombination. The *ahpC* gene is sandwiched between the *ahpD* and *MAB\_4409*. The DNA sequences of the left and right arms of *ahpC* were amplified by PCR and subcloned into pUX1-*katG*. The resulting suicide plasmid was used to transform the strain expressing an additional HA-tagged copy of *ahpC* gene. Dotted lines represent the size (indicated above each line) of the expected PCR products in Mab WT, and  $\Delta$ ahpCe/*ahpCi*-ha. Black arrows represent the primers used for PCR analysis. (B) Tetracycline-mediated regulation of the *ahpC* gene using the tet-OFF configuration in Mab. The *tetR38* gene encoding the T38 repressor is a reverse TetR that recognizes *tetO-4C5G*. Addition of ATc results in binding of T38 to ATc and its recruitment to *tetO-4C5G* represses the transcription of the HA-tagged *ahpCi* gene. T38, Tet repressor; ATc, anhydrotetracycline; *tetO*, Tet operator. (C) PCR analysis confirming the deletion of *ahpC* in  $\Delta$ ahpCe/*ahpCi*-ha. Genomic DNA from Mab was used to amplify the intact *ahpC* locus. Amplicon was subjected to sequencing to confirm the proper deletion of *ahpC*. (D) Time-dependent depletion of the inducible AhpCi-HA upon addition of ATc to the medium is shown after 24 h, 48 h, and 72 h in

DahpCe/ahpCi-ha (upper panel). KasA was used as a loading control (lower panel). (E) Parental Mab and DahpCe/ahpCi-ha strains growth curves in 7H9 media supplemented or not with ATc at 37 °C. The data are from one of two independent experiments. (F) Bacteria were grown to exponential phase and 1.5 mL of 10-fold serial dilutions were spotted onto LB agar medium supplemented or not with 1 mg/ml ATc. Pictures were taken after 5 days of incubation at 37 °C. Arrows indicate the difference of growth in presence or absence of ATc. (G) Comparison of the invasion capacity of the parental and DahpCe/ahpCi-ha strains pre-exposed to 1 mg/mL ATc for 72 h and subsequently used to infect THP-1 cells. CFUs were determined at 3 hpi as reported earlier. The results represent the mean values  $\pm$  GSD of three independent experiments (each conducted in triplicate) (n = 9). One-tailed Tukey's test: ns, non-significant > 0.05, \*\*\*p < 0.001.

## Conditional deletion of ahpC reduces invasion of Mab

Host cell invasion by mycobacteria is dependent on interactions between bacterial adhesins with moonlighting activity and host cell receptors.<sup>37</sup> This may explain why some adhesins are essential for *in vitro* growth. Despite numerous attempts, we were unable to generate an ahpC deletion mutant using the unmarked deletion strategy, previously validated for the deletion of non-essential genes in Mab.<sup>8,38,39</sup> Consequently, to investigate the contribution of AhpC in bacterial uptake by macrophages, we took advantage of the tetracycline repressor system that selectively and ectopically controls gene expression in mycobacteria.<sup>40,41</sup> To generate a conditional ahpC mutant, we introduced the ahpC minigene with a C-terminally positioned HA epitope tag into Mab (Figure 7A). This minigene was placed under the control of the tetracycline regulatory promoter tetO-4C5G and integrated into the bacterial attB locus (designated ahpCi-ha) following selection on hygromycin (Figures 7A and 7B). The resulting ahpCe/ahpCi-ha strain was used to disrupt the endogenous copy of ahpC (designated ahpCe) by double homologous recombination using the pUX1-katG-ahpC vector containing two flanking regions (1009 bp and 1019 bp) of the ahpC gene (Figure 7A). The resulting clones were analyzed by PCR, confirming the proper genotype of the mutant (Figures 7A and 7C). In addition, western blotting was performed to select for clones in which a significant reduction in AhpC-HA expression was observed following treatment with anhydrotetracycline (ATc) (Figure 7D). The knockdown of AhpCi-HA protein in presence of ATc was monitored by western blotting at days 1, 2, and 3 using an anti-HA antibody (Figure 7D). Expression of AhpCi-HA was strongly downregulated in the presence of 1 mg/mL ATc for 72 h (Figure 7D). Based on these observations, all subsequent invasion experiments were conducted using the DahpCe/ahpCi-ha conditional mutant pre-treated with 1 mg/mL ATc for 72 h.

Monitoring bacterial growth failed to show any *in vitro* growth defect on depletion in AhpCi-HA in planktonic cultures during the first 96 h of incubation in the presence of ATc (Figure 7E). However, a more fine-grained growth analysis performed by taking 1.5 mL of the DahpCe/ahpCi-ha culture treated in the presence of 1 mg/mL of ATc showed a slight growth defect on agar plates as evidenced by a decreased number of colonies at the highest dilutions (Figure 7F). As expected, the parental Mab strain grew similarly in the presence or absence of ATc (Figure 7F) whereas in the absence of ATc, the DahpCe/ahpCi-ha mutant grew similarly to the WT strain. This suggests that AhpC is likely to play a minor role for *in vitro* growth. Next, bacteria pre-treated for 72 h with or without ATc were used to infect THP-1 macrophages. At 3 h post-infection, only DahpCe/ahpCi-ha pre-exposed to ATc showed a reduced capacity to invade the cells (Figure 7G). This unambiguously establishes that depletion of AhpC reduces mycobacterial invasion.

## DISCUSSION

Mycobacteria express various PAMP, which directly interact with their cognate PRR, including TLR, CLR, and other receptors.<sup>42</sup> The interplay between macrophages and mycobacteria is complex and is not fully understood. Receptors used by several important human pathogens include tetraspanins, which form adhesion platforms and facilitate internalization of these microorganisms.<sup>22,43–45</sup> Tetraspanins are involved in the pathogenesis of infections caused by viruses, parasites, protozoa and bacteria at various levels.<sup>46</sup> Evidence is accumulating that these membrane proteins are involved in the adhesion and uptake of some bacteria, such as Chlamydia, Listeria or Neisseria<sup>22</sup> whereas their contribution in the recognition of mycobacteria remains unknown. Herein, we demonstrate that tetraspanins participate in the interplay between Mab and host cells, such as macrophages and lung epithelial cells. We showed that tetraspanin CD81 is an abundant protein expressed on the surface of phagocytic and epithelial cells, whereas CD151 is present at the surface of host cells at lower levels.<sup>47,48</sup> We provide compelling evidence that CD81-LEL is crucial for mycobacterial internalization. Interfering with CD81-LEL using neutralizing antibodies caused a significant reduction in Mab uptake by macrophages (THP-1 and primary human macrophages) and pneumocytes. That no inhibition was observed with the LEL of CD151 attests for the specificity of the interaction. Moreover, CD81-LEL-derived peptides considerably reduced the internalization of Mab by macrophages. It is tempting to speculate that these peptides can act similarly to the recombinant CD81-LEL, by preventing the interaction between the bacilli and the macrophage. This is of particular interest given that anti-adherence therapies represent a relatively new area of research to combat infectious diseases.<sup>49</sup> Indeed, most commercially available antimicrobials inhibit the growth of the pathogens but this selective pressure can rapidly lead to the emergence of drug-resistant strains. Unlike traditional drugs, anti-adhesion peptides that target host and bacterial components show a reduced probability of developing resistance.<sup>22,50,51</sup> Small synthetic peptides based on tetraspaninCD9 prevent adhesion of Staphylococcus aureus to human keratinocytes and in a model of human skin.<sup>51</sup> This property, together with their high specificity and low toxicity, make tetraspanin-derived peptides attractive candidates for future antibacterial drug developments.

The requirement of CD81 for optimal internalization of Mab was confirmed by knocking-out CD81-LEL using CRISPR/Cas9 strategy in A549 pneumocytes. Other reports indicate that tetraspanins indirectly contribute to the process of bacterial internalization, either by acting as a co-receptor or by recruiting the receptor to the cell surface via the assembly of tetraspanin-enriched microdomains (TEM) to facilitate bacterial binding.<sup>22</sup> It is very likely that TEM are involved in the adhesion of Salmonella typhimurium to human monocyte-derived macrophage and that this may represent a common mechanism that a variety of bacteria exploit as a mean of attachment before invasion.<sup>52</sup> The inhibitory effect seen on internalization of bacilli when interfering with the CD81-LEL function may be due to the disruption of interactions between cell surface tetraspanins and adhesion receptors, resulting in the disorganization of the adhesion platforms required for optimal bacterial attachment. However, this hypothesis can be dismissed in our study because we have identified, for the first time, a bacterial ligand that interacts directly with the LEL of a tetraspanin in a context where TEM are absent.

Although mass spectrometry analysis identified several putative ligands of CD81-LEL, we primarily focused here on the alkyl hydroperoxide reductase C (AhpC). M. tuberculosis AhpC

belongs to the peroxiredoxin family, acting as a general antioxidant enzyme by reducing alkyl hydroperoxides more effectively than H<sub>2</sub>O<sub>2</sub> and protecting bacilli from oxidative stress.<sup>53</sup> In Mab, AhpC was found to be associated with the cell wall and the cytosolic fractions. Reactive oxygen species and reactive nitrogen intermediates released by phagocytic cells play an important role in the defense against intracellular mycobacteria. It is very likely that AhpC contributes to thwarting the generation of oxidative stress and damage, and consequently protects the bacilli from the oxidative burst, although this needs to be investigated in future studies. In addition, the localization of AhpC on the bacterial surface conceivably facilitates adherence of the bacilli to host cells, where it may act as an adhesin interacting with CD81. Alternately, because of the co-expression of multiple adhesins, blocking one adhesin at a time may not be sufficient to affect the binding of whole bacilli to macrophages. The specificity of the physical interaction between AhpC and CD81 was demonstrated using a combination of in vitro based approaches: (1) Macrophage uptake of AhpC-coated latex beads was higher than that uptake of BSA- or Hsp16.7-coated beads; (2) The uptake of AhpC-coated beads was reduced when macrophages were pre-treated with anti-CD81-LEL antibodies. Thus, these in vitro and in cellulo observations are in good agreement with each other. Future studies should be dedicated

## **Limitations of the study**

Although this study provides meaningful information on the so far unexpected role of surface-associated CD81 during Mab infection, there are some limitations that should be addressed in future studies. For instance, experiments to identify the structural domains involved in the AhpC-CD81-LEL interaction would provide a deeper characterization of this important mechanism of bacterial uptake. Furthermore, because all studies were conducted using ex vivo infected cells, additional work on role of CD81 in the early and late phases of Mab infection should be carried out using mouse models of infection. Because the present work focused essentially on Mab, it would be relevant to explore whether other pathogenic mycobacteria, including *M. tuberculosis*, are also dependent on CD81 during the early interaction and infection with macrophages.

## **STAR+METHODS**

Detailed methods are provided in the online version of this paper and include the following:

### **- KEY RESOURCES TABLE**

### **- RESOURCE AVAILABILITY**

Lead contact

Materials availability

Data and code availability

### **- METHOD DETAILS**

Mycobacterial strains, growth conditions and reagents

Preparation of Mab inocula

Construction of an *ahpC* repressible construct in *M. abscessus*

Generation of the *ahpC* conditional knock-out mutant (*DahpCe/ahpCi-ha*)

In vitro growth assays

Invasion assay of *DahpCe/ahpCi-ha* in macrophages

Overexpression of AhpC and Fmt in *M. abscessus*

Construction of *hsp60*-*Cd81*-LEL-*gfp*-expressing plasmid

Western blotting

Identification of CD81-LEL-GFP protein partners  
Mass spectrometry  
Proteomic data analysis  
Subcellular fractionation of *M. abscessus*  
Cloning of hsp16.7 and ahpC genes in pET30  
Expression and purification of His-tagged Hsp16.7 and AhpC recombinant proteins  
Expression and purification of recombinant CD81-LEL-GST and CD151-LEL-GST  
Macrophage and A549 infection assays  
Infection of primary human monocyte-derived macrophages and intracellular CFU determination  
Immunofluorescence staining of Mab-infected cells  
HA-trap pull-down experiments  
Coating of latex beads with recombinant proteins  
Bead phagocytosis assay  
Antibody inhibition assays in macrophages  
Peptides synthesis  
Characteristics of the peptides used in this study  
Saturating *M. abscessus* AhpC with recombinant CD81-LEL or derived peptides  
Flow cytometry  
CRISPR/Cas9-mediated disruption of Cd81-LEL in A549 cells  
**-QUANTIFICATION AND STATISTICAL ANALYSIS**

## **ACKNOWLEDGMENTS**

This study was supported by the ANR-19-CE15-0012-01 funding (SUNLIVE) and by the Équipe FRMEQU202103012588'' to LK. JK was supported by an Infectiopôle Sud Méditerranée fellowship. We thank the Montpellier RIO Imaging facilities. We are grateful to Pascal Verdié for providing peptide synthesis facilities, Pierre Sanchez for performing LCMS analysis, Pr Dirk Schnappinger for providing us vectors that we used to set up the tet repressible system, Dr Eric Rubinstein for providing us with the pGEX2T vector, and Dr Caroline Goujon and Dr Boris Bonaventure for providing us with the CRISPR-Cas9 material and their know-how to generate the CD81-LEL mutant in A549 cells.

## **AUTHOR CONTRIBUTIONS**

W.D. conceived and conducted experiments, analyzed the data, and wrote the manuscript. J.K., F.B., E.V., P.B., and Y.M.B conducted experiments and analyzed the data. L.K. conceived experiments, acquired funding and amended the manuscript.

# REFERENCES

- Pereira, A.C., Ramos, B., Reis, A.C., and Cunha, M.V. (2020). Non-tuberculous mycobacteria: molecular and physiological bases of virulence and adaptation to ecological niches. *Microorganisms* 8, E1380. <https://doi.org/10.3390/microorganisms8091380>.
- Sharma, S.K., and Upadhyay, V. (2020). Epidemiology, diagnosis & treatment of non-tuberculous mycobacterial diseases. *Indian J. Med. Res.* 152, 185–226. [https://doi.org/10.4103/ijmr.IJMR\\_902\\_20](https://doi.org/10.4103/ijmr.IJMR_902_20).
- Ratnatunga, C.N., Lutzky, V.P., Kupz, A., Doodan, D.L., Reid, D.W., Field, M., Bell, S.C., Thomson, R.M., and Miles, J.I. (2020). The rise of non-tuberculosis mycobacterial lung disease. *Front. Immunol.* 11, 303. <https://doi.org/10.3389/fimmu.2020.00303>.
- Hannah, C.E., Ford, B.A., Chung J., Ince, D., and Wanat, K.A. (2020). Characteristics of non-tuberculous mycobacterial infections at a midwestern tertiary hospital: a retrospective study of 365 patients. *Open Forum Infect. Dis.* 7, ofaa173. <https://doi.org/10.1093/ofid/ofaa173>.
- Johansen, M.D., Herrmann, J.-L., and Kremer, L. (2020). Non-tuberculous mycobacteria and the rise of *Mycobacterium abscessus*. *Nat. Rev. Microbiol.* 18, 392–407. <https://doi.org/10.1038/s41579-020-0331-1>.
- To, K., Cao, R., Yegiazaryan, A., Owens, J., and Venketaraman, V. (2020). General overview of non-tuberculous mycobacteria opportunistic pathogens: *Mycobacterium avium* and *Mycobacterium abscessus*. *J. Clin. Med.* 9, E2541. <https://doi.org/10.3390/jcm9082541>.
- Dubois, V., Pawlik, A., Bories, A., Le Moigne, V., Simeira, O., Legendre, R., Varet, H., Rodríguez-Ordóñez, M.D.P., Gaillard, J.-L., Coppée, J.Y., et al. (2019). *Mycobacterium abscessus* virulence traits unraveled by transcriptomic profiling in amoeba and macrophages. *PLoS Pathog.* 15, e1008069. <https://doi.org/10.1371/journal.ppat.1008069>.
- Daher, W., Ledercq, L.-D., Johansen, M.D., Hamela, C., Karam, J., Trivelli, X., Nigou, J., Guérardel, Y., and Kremer, L. (2022). Glycopeptidolipid glycosylation controls surface properties and pathogenicity in *Mycobacterium abscessus*. *Cell Chem. Biol.* 29, 910–924.e7. <https://doi.org/10.1016/j.chembiol.2022.03.008>.
- Kim, B.-R., Kim, B.-J., Kook, Y.-H., and Kim, B.-J. (2019). Phagosome escape of rough *Mycobacterium abscessus* strains in murine macrophage via phagosomal rupture can lead to type I interferon production and their cell-to-cell spread. *Front. Immunol.* 10, 125. <https://doi.org/10.3389/fimmu.2019.00125>.
- Kim, B.-R., Kim, B.-J., Kook, Y.-H., and Kim, B.-J. (2020). *Mycobacterium abscessus* infection leads to enhanced production of type I interferon and NLRP3 inflammasome activation in murine macrophages via mitochondrial oxidative stress. *PLoS Pathog.* 16, e1008294. <https://doi.org/10.1371/journal.ppat.1008294>.
- Le Moigne, V., Roux, A.-L., Jobart-Malfait, A., Blanc, L., Chaoui, K., Buriel-Schiltz, O., Gaillard, J.-L., Canaan, S., Nigou, J., and Herrmann, J.-L. (2020). A TLR2-activating fraction from *Mycobacterium abscessus* rough variant demonstrates vaccine and diagnostic potential. *Front. Cell. Infect. Microbiol.* 10, 432. <https://doi.org/10.3389/fcimb.2020.00432>.
- Malcolm, K.C., Caceres, S.M., Pohl, K., Poch, K.R., Bernut, A., Kremer, L., Bratton, D.L., Herrmann, J.-L., and Nick, J.A. (2018). Neutrophil killing of *Mycobacterium abscessus* by intra- and extracellular mechanisms. *PLoS One* 13, e0196120. <https://doi.org/10.1371/journal.pone.0196120>.
- Ryan, K., and Byrd, T.F. (2018). *Mycobacterium abscessus*: shapeshifter of the mycobacterial world. *Front. Microbiol.* 9, 2642. <https://doi.org/10.3389/fmicb.2018.02642>.
- Zhang, C., Asif, H., Holt, G.E., Griewald, A.J., Campos, M., Bejano, P., Fregien, N.L., and Mirsaeidi, M. (2019). *Mycobacterium abscessus*-bronchial epithelial cells cross-talk through type I interferon signaling. *Front. Immunol.* 10, 2888. <https://doi.org/10.3389/fimmu.2019.02888>.
- Roux, A.-L., Viljoen, A., Bah, A., Simeone, R., Bernut, A., Laencina, L., Demauidt, T., Rottman, M., Gaillard, J.-L., Majlessi, L., et al. (2016). The distinct fate of smooth and rough *Mycobacterium abscessus* variants inside macrophages. *Open Biol.* 6, 160185. <https://doi.org/10.1098/rsob.160185>.
- Shamsi, M., and Mirsaeidi, M. (2021). Non-tuberculous mycobacteria, macrophages, and host innate immune response. *Infect. Immun.* 89, e0081220. <https://doi.org/10.1128/IAI.00812-20>.
- Tran, T., Bonham, A.J., Chan, E.D., and Honda, J.R. (2019). A paucity of knowledge regarding non-tuberculous mycobacterial lipids compared to the tubercle bacillus. *Tuberculosis* 115, 96–107. <https://doi.org/10.1016/j.tube.2019.02.008>.
- Liu, C.H., Liu, H., and Ge, B. (2017). Innate immunity in tuberculosis: host defense vs pathogen evasion. *Cell. Mol. Immunol.* 14, 963–975. <https://doi.org/10.1038/cmi.2017.88>.
- Upadhyay, S., Mittal, E., and Philips, J.A. (2018). Tuberculosis and the art of macrophage manipulation. *Pathog. Dis.* 76, fy037. <https://doi.org/10.1093/femspd/fy037>.
- Lee, H.-J., Woo, Y., Hahn, T.-W., Jung, Y.M., and Jung, Y.-J. (2020). Formation and maturation of the phagosome: a key mechanism in innate immunity against intracellular bacterial infection. *Microorganisms* 8, E1298. <https://doi.org/10.3390/microorganisms8091298>.
- Ribeiro, G.M., Matsumoto, C.K., Real, F., Teixeira, D., Duarte, R.S., Morbara, R.A., Leão, S.C., and de Souza Carvalho-Wodarz, C. (2017). Increased survival and proliferation of the epidemic strain *Mycobacterium abscessus* subsp. *massiliense* CRM0019 in alveolar epithelial cells. *BMC Microbiol.* 17, 195. <https://doi.org/10.1186/s12866-017-1102-7>.
- Karam, J., Méresse, S., Kremer, L., and Daher, W. (2020). The roles of tetraspanins in bacterial infections. *Cell Microbiol.* 22, e13260. <https://doi.org/10.1111/cmi.13260>.
- Hemler, M.E. (2008). Targeting of tetraspanin proteins—potential benefits and strategies. *Nat. Rev. Drug Discov.* 7, 747–758. <https://doi.org/10.1038/nrd2659>.
- Homsy, Y., Schloetel, J.-G., Scheffer, K.D., Schmidt, T.H., Destainville, N., Florin, L., and Lang, T. (2014). The extracellular  $\beta$ -domain is essential for the formation of CD81 tetraspanin webs. *Biophys. J.* 107, 100–113. <https://doi.org/10.1016/j.bpj.2014.05.028>.
- Huang, Y., and Yu, L. (2022). Tetraspanin-enriched microdomains: the building blocks of migasomes. *Cell Insight* 1, 100003. <https://doi.org/10.1016/j.cellin.2021.100003>.
- Kumar, A., Hossain, R.A., Yost, S.A., Bu, W., Wang, Y., Dearborn, A.D., Grakoui, A., Cohen, J.I., and Marcotrigiano, J. (2021). Structural insights into hepatitis C virus receptor binding and entry. *Nature* 598, 521–525. <https://doi.org/10.1038/s41586-021-03913-5>.
- Gordón-Alonso, M., Yañez-Mó, M., Barreiro, O., Álvarez, S., Muñoz-Fernández, M.A.,

- Valenzuela-Fernández, A., and Sánchez-Madrid, F. (2006). Tetraspanins CD9 and CD81 modulate HIV-1-induced membrane fusion. *J. Immunol.* 177, 5129–5137. <https://doi.org/10.4049/jimmunol.177.8.5129>.
28. Sívie, O., Rubinstein, E., Franetich, J.-F., Prenant, M., Belnoue, E., Rénia, L., Hannoun, L., Eling, W., Levy, S., Bouchek, C., and Mazier, D. (2003). Hepatocyte CD81 is required for *Plasmodium falciparum* and *Plasmodium yoelii* sporozoite infectivity. *Nat. Med.* 9, 93–96. <https://doi.org/10.1038/nm808>.
29. Tham, T.N., Gouin, E., Rubinstein, E., Bouchek, C., Cossart, P., and Pizarro-Cerda, J. (2010). Tetraspanin CD81 is required for *Listeria monocytogenes* invasion. *Infect. Immun.* 78, 204–209. <https://doi.org/10.1128/IAI.00661-09>.
30. Astarfo-Dequeker, C., N'Diaye, E.N., Le Cibeac, V., Rittig, M.G., Prand, J., and Maridonneau-Parrini, I. (1999). The mannose receptor mediates uptake of pathogenic and non-pathogenic mycobacteria and bypasses bactericidal responses in human macrophages. *Infect. Immun.* 67, 469–477. <https://doi.org/10.1128/IAI.67.2.469-477.1999>.
31. Fratuzzi, C., Marjunath, N., Arbeit, R.D., Carini, C., Gekker, T.A., Ardman, B., Remold-O'Donnell, E., and Remold, H.G. (2000). A macrophage invasion mechanism for mycobacteria implicating the extracellular domain of CD43. *J. Exp. Med.* 192, 183–192. <https://doi.org/10.1084/jem.192.2.183>.
32. Herford, G., and Wiker, H.G. (1994). Antigen 85C on *Mycobacterium bovis*, BCG and *M. tuberculosis* promotes monocyte-CR3-mediated uptake of microbeads coated with mycobacterial products. *Immunology* 82, 445–449.
33. Hiday, T.B.M., Zitener, H.J., Speert, D.P., and Stokes, R.W. (2010). *Mycobacterium tuberculosis* employs Cpn60.2 as an adhesin that binds CD43 on the macrophage surface. *Cell Microbiol.* 12, 1634–1647. <https://doi.org/10.1111/j.1462-5822.2010.01496.x>.
34. Sendide, K., Rainer, N.E., Lee, J.S.I., Bourgoin, S., Talal, A., and Hama, Z. (2005). Cross-talk between CD14 and complement receptor 3 promotes phagocytosis of mycobacteria: regulation by phosphatidylinositol 3-kinase and cytohesin-1. *J. Immunol.* 174, 4210–4219. <https://doi.org/10.4049/jimmunol.174.7.4210>.
35. Doyle, T., Mancorgé, O., Bonaventura, B., Polpeter, D., Lusegnol, M., Taziet, M., Apolonia, L., Catanese, M.-T., Goujon, C., and Malm, M.H. (2018). The interferon-inducible isoform of NCOA7 inhibits endosome-mediated viral entry. *Nat. Microbiol.* 3, 1369–1376. <https://doi.org/10.1038/s41564-018-0273-9>.
36. Master, S.S., Springer, B., Sander, P., Boettger, E.C., Denic, V., and Timmins, G.S. (2002). Oxidative stress response genes in *Mycobacterium tuberculosis*: role of *ahpC* in resistance to peroxynitrite and stage-specific survival in macrophages. *Microbiology* (Read) 148, 3139–3144. <https://doi.org/10.1099/00222728-148-10-3139>.
37. Kumar, S., Puniya, B.L., Parween, S., Nahar, P., and Ramchandran, S. (2013). Identification of novel adhesins of *M. tuberculosis* H37Rv using integrated approach of multiple computational algorithms and experimental analysis. *PLoS One* 8, e69790. <https://doi.org/10.1371/journal.pone.0069790>.
38. Daher, W., Lederer, L.-D., Vijoen, A., Karam, J., Dufrene, Y.F., Guarandé, Y., and Kramer, L. (2020). O-methylation of the glycopeptidolipid acyl chain defines surface hydrophobicity of *Mycobacterium abscessus* and macrophage invasion. *ACS Infect. Dis.* 6, 2756–2770. <https://doi.org/10.1021/acinfed.0c00490>.
39. Richard, M., Gutiérrez, A.V., Vijoen, A., Rodríguez-Rincon, D., Roquet-Baneres, F., Blaise, M., Eversil, L., Parkhill, J., Floto, R.A., and Kramer, L. (2019). Mutations in the MAB\_2299c TetR regulator confer cross-resistance to clofazimine and bedaquiline in *Mycobacterium abscessus*. *Antimicrob. Agents Chemother.* 63, e01316–e01318. <https://doi.org/10.1128/AAC.01316-18>.
40. Eht, S., Guo, X.V., Hickey, C.M., Ryou, M., Monteleone, M., Riley, L.W., and Schnappinger, D. (2005). Controlling gene expression in mycobacteria with anhydrotetracycline and Tet repressor. *Nucleic Acids Res.* 33, e21. <https://doi.org/10.1093/nar/gni013>.
41. Kim, J.-H., O'Brien, K.M., Sharma, R., Boshoff, H.I.M., Rahnen, G., Chakraborty, S., Wallach, J.B., Monteleone, M., Wilson, D.J., Aldrich, C.C., et al. (2013). A genetic strategy to identify targets for the development of drugs that prevent bacterial persistence. *Proc. Natl. Acad. Sci. USA* 110, 19095–19100. <https://doi.org/10.1073/pnas.1315860110>.
42. Vnod, V., Vijayarajam, S., Vasudevan, A.K., and Bawa, R. (2020). The cell surface adhesins of *Mycobacterium tuberculosis*. *Microbiol. Res.* 232, 126392. <https://doi.org/10.1016/j.micres.2019.126392>.
43. Hantak, M.P., Qing, E., Earnest, J.T., and Gallagher, T. (2019). Tetraspanins: architects of viral entry and exit platforms. *J. Virol.* 93, 014299–17–e1517. <https://doi.org/10.1128/JVI.01429-17>.
44. Manzoni, G., Marfnach, C., Topçu, S., Briquet, S., Grand, M., Tolle, M., Gransagne, M., Lescar, J., Andolina, C., Franetich, J.-F., et al. (2017). *Plasmodium* P36 determines host cell receptor usage during sporozoite invasion. *Elife* 6, e25903. <https://doi.org/10.7554/eLife.25903>.
45. New, C., Lee, Z.-Y., Tan, K.S., Wong, A.H.-P., Wang, D.Y., and Tran, T. (2021). Tetraspanins: host factors in viral infections. *Int. J. Mol. Sci.* 22, 11609. <https://doi.org/10.3390/ijms22111609>.
46. van Spruiel, A.B., and Figdor, C.G. (2010). The role of tetraspanins in the pathogenesis of infectious diseases. *Microb. Infect.* 12, 106–112. <https://doi.org/10.1016/j.micinf.2009.11.001>.
47. Green, L.R., Monk, P.N., Partridge, L.J., Morris, P., Goringe, A.R., and Read, R.C. (2010). Cooperative role for tetraspanins in adhesion-mediated attachment of bacterial species to human epithelial cells. *Infect. Immun.* 79, 2241–2249. <https://doi.org/10.1128/IAI.01354-10>.
48. Raynaud, C., Daher, W., Johansen, M.D., Roquet-Baneres, F., Blaise, M., Onajole, O.K., Kozikowski, A.P., Hermann, J.-L., Dziadek, J., Gobi, K., and Kramer, L. (2020). Active benzimidazole derivatives targeting the MmpL3 transporter in *Mycobacterium abscessus*. *ACS Infect. Dis.* 6, 324–337. <https://doi.org/10.1021/acinfed.9b00389>.
49. Asadi, A., Razzavi, S., Talebi, M., and Gholami, M. (2019). A review on anti-adhesion therapies of bacterial diseases. *Infection* 47, 13–23. <https://doi.org/10.1007/s15010-018-1222-5>.
50. Robert, J.-M.H., Amoussou, N.G., Maï, H.L., Logé, C., and Brouard, S. (2021). Tetraspanins: useful multifunction proteins for the possible design and development of small-molecule therapeutic tools. *Drug Discov. Today* 26, 56–68. <https://doi.org/10.1016/j.drudis.2020.10.022>.
51. Ventres, J.K., Partridge, L.J., Read, R.C., Cozens, D., MacNeil, S., and Monk, P.N. (2016). Peptides from tetraspanin CD9 are potent inhibitors of *Staphylococcus aureus* adherence to keratinocytes. *PLoS One* 11, e0160887. <https://doi.org/10.1371/journal.pone.0160887>.
52. Hasuna, N.A., Monk, P.N., Ali, F., Read, R.C., and Partridge, L.J. (2017). A role for the tetraspanin proteins in *Salmonella* infection of human macrophages. *J. Infect.* 75, 115–124. <https://doi.org/10.1016/j.jinf.2017.06.003>.
53. Guimarães, B.G., Souchon, H., Honoré, N., Saint-Joanis, B., Brosch, R., Shepard, W., Cole, S.T., and Alzari, P.M. (2005). Structure and mechanism of the alkylhydroperoxidase AlpC, a key element of the *Mycobacterium tuberculosis* defense system against oxidative stress. *J. Biol. Chem.* 280, 25735–25742. <https://doi.org/10.1074/jbc.M503076200>.
54. Israeli, S.J., and McMillan-Ward, E.M. (2007). Platelet tetraspanin complexes and their association with lipid rafts. *Thromb. Haemostasis* 98, 1081–1087.
55. Berditchevski, F. (2001). Complexes of tetraspanins with integrins: more than meets the eye. *J. Cell Sci.* 114, 4143–4151. <https://doi.org/10.1242/jcs.114.23.4143>.
56. Kummer, D., Steinbacher, T., Schwitzer, M.F., Tholmann, S., and Ebner, K. (2020). Tetraspanins: integrating cell surface receptors to functional microdomains in homeostasis and disease. *Med. Microbiol. Immunol.* 209, 397–405. <https://doi.org/10.1007/s00430-020-00673-3>.
57. Termini, C.M., and Gillete, J.M. (2017). Tetraspanins function as regulators of cellular signaling. *Front. Cell Dev. Biol.* 5, 34. <https://doi.org/10.3389/fcell.2017.00034>.

